Cent. Eur. J. Chem. • 8(5) • 2010 • 1041–1046
DOI: 10.2478/s11532-010-0073-4

VERSITA

Central European Journal of **Chemistry**

# Effect of the polymeric coating over $Fe_3O_4$ particles used for magnetic separation

**Research Article**

Raúl Terrazas Reza[1], Carlos A. Martínez Pérez[1], Claudia A. Rodríguez González[1], Humberto Monreal Romero[2], Perla E. García Casillas[1*]

[1]*Institute of Engineering and Technology, Autonomous University of Juarez City, C.P. 32320, Juarez City, Mexico*

[2]*Autonomous University of Chihuahua, C.P. 3100, Chihuahua, Mexico*

**Received 16 December 2009; Accepted 7 May 2010**

**Abstract:** In this work, the synthesis of magnetite nanoparticles by two variant chemical coprecipitation methods that involve reflux and aging conditions was investigated. The influence of the synthesis conditions on particle size, morphology, magnetic properties and protein adsorption were studied. The synthesized magnetite nanoparticles showed a spherical shape with an average particle size directly influenced by the synthesis technique. Particles of average size 27 nm and 200 nm were obtained. When the coprecipitation method was used without reflux and aging, the smallest particles were obtained. Magnetite nanoparticles obtained from both methods exhibited a superparamagnetic behavior and their saturation magnetization was particle size dependent. Values of 67 and 78 emu $g^{-1}$ were obtained for the 27 nm and 200 nm magnetite particles, respectively. The nanoparticles were coated with silica, aminosilane, and silica-aminosilane shell. The influence of the coating on protein absorption was studied using Bovine Serum Albumin (BSA) protein.

**Keywords:** *Chemical coprecipitation • Magnetic separation • Biofunctional nanoparticles • Bovine serum albumin (BSA) • Protein adsorption*



## 1. Introduction

Nanometer-sized particles have been proved to be more efficient in different magnetic applications than micrometric particles [1-2]. At the nanoscale, each particle contains a simple magnetic domain and shows a superparamagnetic behavior. Many nanoparticles of this type are metallic, which are not stable and can be easily oxidized, thus their applications are limited. On the other hand, metallic oxides overcome these problems and can be applied in many different fields. Magnetite ($Fe_3O_4$) has been widely used in the field of magnetic materials [3-4]. The magnetic nanoparticles have been coated with different functional materials for specific applications. Among the most utilized superficial functional groups are aldehyde (-CHO), hydroxyl (-OH), amines ($-NH_2$), and others [5-10]. The addition of these functional groups onto magnetic nanoparticles allows the attachment of bioactive materials to their surfaces. Great advantages can be achieved due to the fact that activated magnetic nanoparticles can be manipulated in the magnetic field. One application of these nanoparticles is to isolate and purify different types of proteins and peptides [11]. The basic principle of the magnetic separation is simple. Magnetic carriers are coated with organic coatings which contain active functional groups that are biocompatible. Hence they can be conjugated with biomolecules such as proteins and antibodies, and

* *E-mail: pegarcia@uacj.mx*
*perlaelviagarcia@yahoo.com*

isolated by applying an external magnetic field.

The synthesis of magnetic particles of uniform size and desired shape is a very important step towards their further surface activation and applications [12-16]. In this paper, the synthesis of magnetite nanoparticles and the effect of the different coating on the capacity for protein adsorption are presented.

# 2. Experimental Procedure

## 2.1. Synthesis of magnetite nanoparticles

### *2.1.1. Chemical Coprecipitation*

For the synthesis of magnetite particles, 1.351 g of Ferric Chloride ($FeCl_3$•$6H_2O$ CAS No. 10025-77-1) and 0.6852 g of Ferrous Sulphate ($FeSO_4$•$7H_2O$ CAS No. 7782-63-0) were mixed with 25 mL deionized water, then ammonium hydroxide ($NH_4OH$ CAS No. 1336-21-6) was added dropwise until a precipitate was formed. In order to remove the residual ions, the obtaining precipitate was centrifuged and washed several times until a pH value of 7 was obtained; the powder was dried at 100°C for 2 hours.

### *2.1.2. Method of Coprecipitation with reflux and aging*

Two different solutions were prepared to synthesize magnetite nanoparticles. In the first one, Ferric Chloride- $FeCl_3.6H_2O$ CAS No. 10025-77-1 (1.351 g) was dissolved in deionized water (10 mL), and then placed in a flask with reflux condenser; this solution was heated up to 80°C for 2 h in order to form FeOOH particles. The solution was cooled down to room temperature and the obtained precipitate was isolated by means of centrifugation. This precipitate was dissolved in water (10 mL). In the second solution, Ferrous Sulphate- $FeSO_4$•$7H_2O$ CAS No. 7782-63-0 (0.6852 g) and Urea-$NH_2CONH_2$ CAS No. 57-13-6 (2.1 g) were dissolved in water (15 mL). Both solutions were transferred to a flask with reflux conditions and mixed. This mixture was then heated up to 90°C in 20 h in order to form magnetite nanoparticles. The obtained precipitate was then centrifuged and washed several times with deionized water until a pH value of 7 was obtained and residual ions was removed; the precipitate was dried at 35°C for 24 h.

## 2.2. Aminosilane Coating

The aminosilane shell was obtained by dissolving N-(2-aminoethyl)-3aminopropyltrimetoxysilane CAS No 1760-24-3 (100 µL), magnetic nanoparticles (0.02 g) and deionized water (25 µL) in Methanol CAS 67-56-1(2.5 mL). The mixture was exposed to ultrasonic agitation for 30 minutes. After that, glycerol (1.5 mL) was added, and the solution was heated up to 90°C, while reaching a maximum mechanical agitation. This temperature and agitation conditions were kept for 6 h. The obtained precipitate was washed with water and Methanol for 4 times in each case.

## 2.3. Silica-Aminosilane Coating

The nanoparticles were coated in two steps: first, a Silica coating was applied using the method proposed by Liu et al. with slight modifications [8]. Sodium Metasilicate CAS No. 6834-92-0 (0.1910 g) was dissolved in deionized water (10 mL), and then nanoparticles (0.020 g) were added. The mixture was subjected to ultrasonic agitation for 30 minutes, and then heated up to 80°C. At this temperature, the pH of the solution was lowered to 6 using HCl CAS No. 9004-54-50 and titrating dropwise. The nanoparticles were washed several times until a pH of 7 was obtained. This procedure was repeated twice. Finally, the powder was dried at 35°C for 24 hours. In the second step, an additional shell of aminosilane was adhered following the process from section 2.2.

## 2.4. Protein immobilization

The protein immobilization over magnetite nanoparticles was evaluated using four different surface conditions: pure magnetite –no coating- (M sample), magnetite with silica coating (M-S sample), magnetite with aminosilane coating (M-A sample) and magnetite with silica and aminosilane coatings (M-S-A sample).

Bovine Serum Albumin (BSA) CAS No. 9048-46-8 was used as standard protein. A BSA solution with a concentration of 2 µg $\mu L^{-1}$ was prepared by dissolving BSA (40 µg) in JAW™ Tris Buffered Saline (TBS) (20 µL). During each protein adsorption experiment, a calibration curve was obtained as the BSA concentrations going from 0 to 2.0 µg $\mu L^{-1}$, with increments of 0.2 µg $\mu L^{-1}$.

Glutaraldehyde CAS No. 111-30-8(15 mL) was added to the particles and they were agitated ultrasonically for 45 minutes before the nanoparticles were mixed with the BSA. The protein immobilization was achieved by mixing nanoparticles (10 µg) with different initial concentrations of BSA in a total volume of 300 µL. The incubating process was under room temperature, with vigorous continuous agitation (Vortex®) and for a time period of 30 minutes. Subsequently, the amount of protein immobilization was determined by measuring the protein loss in the solution. The protein concentration in the BSA solution was determined by the Bradford colorimetric method at a visible wavelength of 595 nm. Micro-plaques, Bradford reagents and a visible light

spectrometer BIO RAD® Benchmark plus were used. 5 µL of incubated solution was transferred to the micro-plaque and 250 µL of Bradford reagent was added. Then, samples were measured in the spectrometer. Three samples were measured for each condition.

### 2.5. Characterization

X-Ray Diffraction (XRD) was used to confirm the magnetite ($Fe_3O_4$) phase. The size distribution and morphology of nanoparticles with and without coating were characterized by Field Emission Scanning Electron Microscope (FESEM). Fourier Transform Infrared Spectroscopy (FTIR) was used in order to confirm the adherence of the polymeric shell through band detection. The magnetic properties such as saturation magnetization and coercivity were obtained using a Vibrating Sample Magnetometer (VSM). Protein adsorption on magnetite nanoparticles was determined by a Visible Light Spectrometer.

## 3. Results and Discussion

Magnetite obtained by coprecipitation with reflux and aging processes showed larger particle size than the magnetite obtained without them. The Fig. 1 shows the images of the magnetite nanoparticles and their size distribution for each sample. The obtained magnetite nanoparticles were spherical in both methods. For the chemical coprecipitation method, the particle size was 27 nm ± 8 nm. For the reflux and aging method, the average particle size was 206 nm ± 58 nm. According to the results, the magnetite obtained by chemical coprecipitation showed smaller average particle size and better size uniformity than the magnetite obtained from reflux and aging method. This can be established by comparing the standard deviations of the two particle size distributions.

The XRD patterns of the synthesized nanoparticles by two methods are shown in Fig. 2. In both cases an inverse spinel crystal structure was obtained, which corresponds to the magnetite structure. The obtained XRD patterns showed differences in the peak width, which is due to the different crystallite size. Wide peaks indicate the small crystals, as in chemical coprecipitation, while the narrow ones indicate larger crystals as in reflux and aging method.

The coating of the particles was confirmed through FTIR spectra (Fig. 3). The magnetite particles (M) show the characteristic band of Fe-O bond at 590 $cm^{-1}$ approximately. When the particles of magnetite are coated with aminosilane (MA) bands at 3309 and 1654 $cm^{-1}$ were observed, which are attributed to the amine group ($-NH_2$) [17]. The band at 2943 $cm^{-1}$ is due to the stretching of C-H from methyl group ($-CH_2$, $-CH_3$). Coated samples show a band at 1072 $cm^{-1}$ which is due to the Si-O bond. When the particles have a silica shell (Silica-Aminosilane Coating-MAS sample), a new band is shown at 802 $cm^{-1}$ due to Si-O-Si bond [18]. The same band was found in both methods of magnetite synthesis, which demonstrates that the Silica-Aminosilane union has taken place.

The suggested mechanism of coated particles is shown in Scheme 1. In magnetite-aminosilane shell, the silicon was bonded with the iron through the deprotonation of magnetite. When a silica shell is added before the aminosilane groups, the silicon is bonded in the same way with the magnetite and silicon bonded with aminosilane through S-O-S bond.

The hysteresis loops were obtained for the magnetite with and without coating. In both methods the nanoparticles exhibited a superparamagnetic behavior (Fig. 4). The saturation magnetization of the coated particles is smaller than that of uncoated magnetite. Aminosilane coating had less impact on the saturation magnetization, while the silica-aminosilane coatings showed a greater effect on this property. Results are shown in Fig. 5.

The amount of Albumin Serum Bovine (BSA) protein immobilized onto nanoparticles surface is influenced by the type of coating present, and in all cases it is superior to that observed for uncoated magnetite.

All types of coatings have the amine functional group ($-NH_2$). Samples of MA and MSA, had higher capacity for protein adherence than pure magnetite (no coating). MSA showed a maximum protein retention capacity of 9.83 µg ASB/ µg nanoparticles, which is higher than the protein capacity of 7.18 µg ASB/ µg nanoparticles for MA. Fig. 6 shows the dependence of protein adsorption on the amount of BSA added. It can be observed that adsorption capacity increases until it reaches a

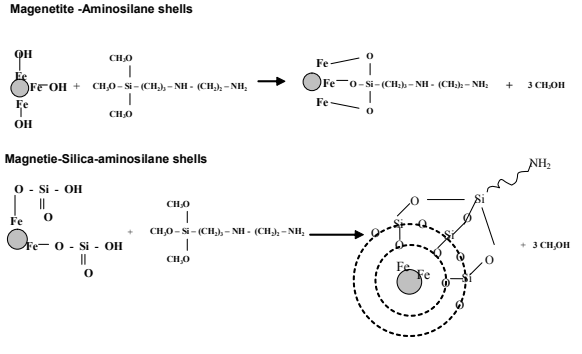


**Scheme 1.** Suggested mechanism of coated magnetite nanoparticles.

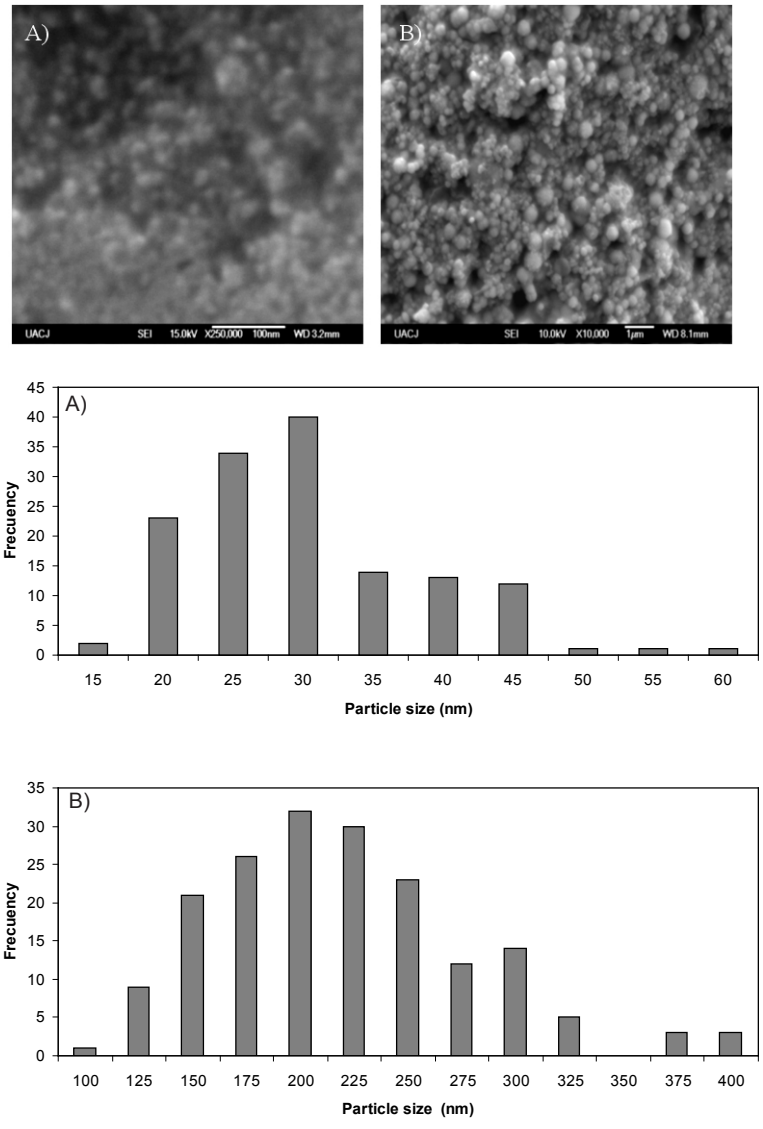


**Figure 1.** Micrograph and particle size distribution of magnetite particles obtained by A) chemical coprecipitation and B) chemical with reflux and aging.

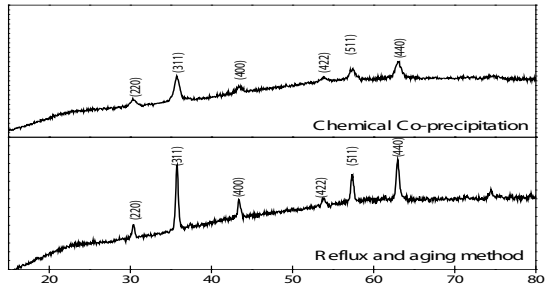


**Figure 2.** XRD of magnetite obtained by chemical coprecipitation and reflux and aging method.

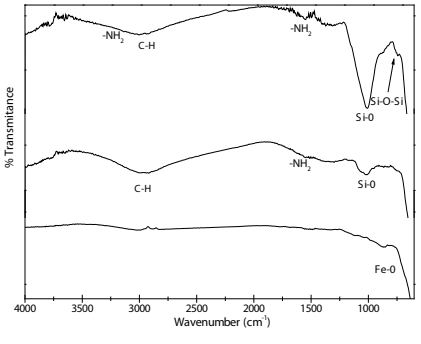


**Figure 3.** FTIR of magnetite (M), magnetite-aminosilane (MA) and magnetite-silica-aminosilane (MSA) obtained by reflux and aging method.

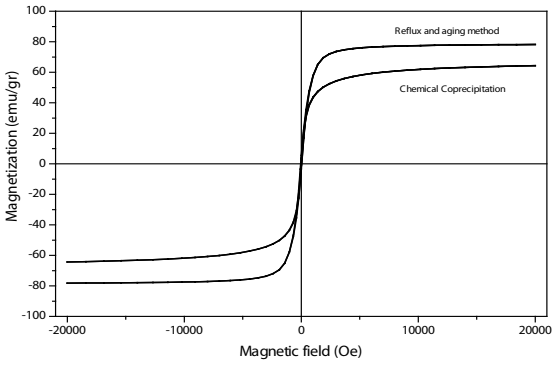


**Figure 4.** Hysteresis loop of magnetite obtained by chemical + coprecipitation and reflux and aging method.

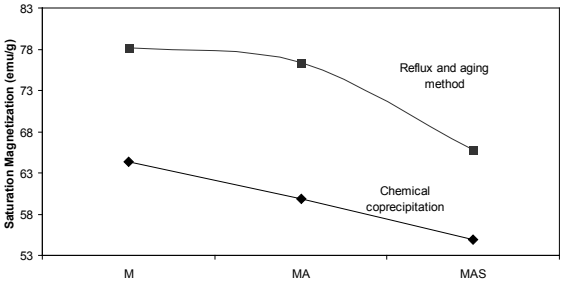


**Figure 5.** Saturation magnetizations of coated and uncoated magnetite nanoparticles.

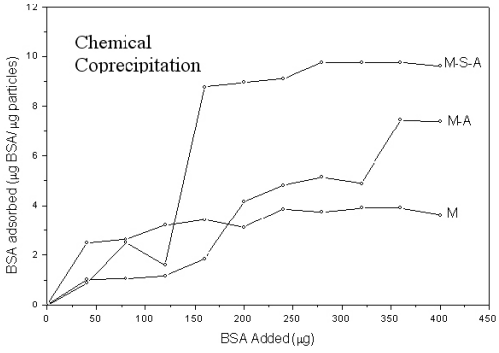


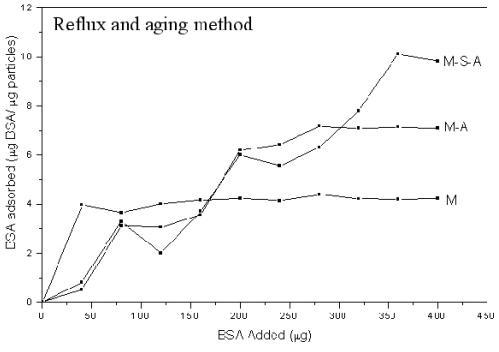


**Figure 6.** Dependence of protein adsorption on the amount of BSA added to the nanoparticles obtained by chemical coprecipitation and reflux and aging method.

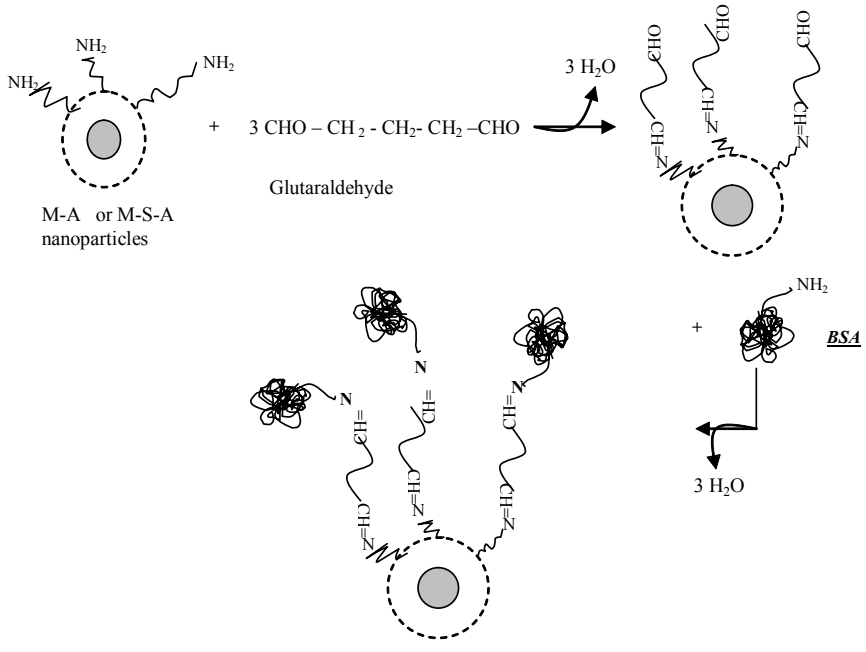


**Scheme 2.** Suggested mechanism of coated magnetite nanoparticles.

saturation state (no more protein is adsorbed).

This was confirmed in this research, and it was found that magnetite nanoparticles coated with silica-aminosilane (MSA) exhibit higher protein immobilization capacity than magnetite coated with aminosilane (MA). Although both types of coatings have the amine functional group on their chains, the observed difference in protein adsorption between MA and MSA samples is explained by the differences in particle stabilization. Nanoparticles usually agglomerate due to their magnetic nature. The first coating with sodium metasilicate stabilizes the particles and diminishes the agglomeration which increases the particle surface area. Therefore, the second coating is more homogenous and consequently, the aminosilane bond and the BSA adsorption increased [19].

The observed results for the BSA protein immobilization can be explained as follows: According to Guoxin *et al.* [20] the amine functional group can be transferred into aldehyde group (glutaraldehyde activation) and conjugated to BSA protein (Scheme 2).

## 4. Conclusions

The coatings on the magnetite nanoparticles surface significantly improved the protein adsorption capacity with no detriment of their superparamagnetic behavior. A fast magnetization and demagnetization was observed when an external magnetic field was applied and removed, respectively. The type of functional group presenting in the coatings and their stability influence the protein adsorption property of the coated particles. The magnetite with silica-aminosilane coating showed the highest protein adsorption capacity due to the presence of the amine functional group in the coating and the highest surface adherence of the coating array.

## Acknowledgement

The authors gratefully acknowledge the Science and Technology Council of México for the financial support granted to this project (CONACYT SEP-2004-C01-47290).

### References

[1] A. Lu, E.L. Salabas, F. Schuth, Angew Chem. 46, 8 (2007)
[2] G. Schmid, Nanoparticles: From Theory to Application, 1st edition (Wiley-VCH Verlag GmbH Co. KGaA, Weinheim, 2004)
[3] G. Cao, Nanostructures & Nanomaterials: Synthesis, Properties & Applications, (Imperial College Press, London, 2004).
[4] R.M. Cornell, U. Schwertmann, The iron oxides: Structure, Properties, Reactions, Occurrences and Uses, Second edition (Willey-VCH GmbH & Co. Egaa, New York, 2003)
[5] C. Yu, K. Tam, C. Lo, S. Tsang, IEEE Trans. Magn. 43, 6 (2007)
[6] M. Yamaura, R. Camilo, L. Sampaio, M. Macedo, M. Nakamura, H. Toma, J. Magn. Magn. Mater. 279, 2 (2004)
[7] J. Xing, B. Zhang, Y. Lang, Y.H. Liu, H. Sci. China Ser. B 51, 2 (2008)
[8] X. Liu, Z. Ma, J. Xing, H. Liu, J. Magn. Magn. Mater. 270, 12 (2004)
[9] M. Ma, Y. Zhang, W. Yu, H. Shen, H. Zhang, N. Gu. Colloid Surf. A: Phys. Eng. Aspects 212, 2 (2003)
[10] B. Kobayashi, S. Saeki, M. Yoshida, D. Nagao, M. Konno, Springer Science+Business Media, LLC, DOI: 10.1007/s10971-007-1648-1
[11] I. Safarik, M. Safarikova, BioMagnetic Res. Tech. DOI: 10.1186/1477-04X-2-7.
[12] G. Gnanaprakash, S. Mahadevan, T. Jayakumar, P. Kalyanasundaram, J. Philip, R. Baldev, Mater. Chem. Phys. 103, 168 (2007)
[13] Q. Chen, J. Wang, Y. Xiong, M. Wu, Z. Peng, Chem. Lett. 34, 5 (2005)
[14] J. Wang, A. Peng, Y. Huang, Q. Chen, J. Cryst. Growth, 263, 616 (2004)
[15] P. Yang, J. Yu, T. Wu, G. Liu, T. Chang, D. Lee, D. Cho, Chinese Chem. Lett. 15, 1 (2004)
[16] B. Zhang, J. Xing, H Liu, Chem. Eng. China. 1, 1 (2007)
[17] H. Günzler, H. GremLich, IR Spectroscopy, 2nd edtion (Wiley-VCH, Germany, 2002)
[18] Y. Ivanova, Ts. Gerganova, H.M.H.V. Fernandes, I.M. Miranda, E. Kashchieva, J. Univ. Chem. Metal. 41, 3 (2006)
[19] I.J. Bruce, J. Taylor, M. Todd, M.J. Davies, E. Borioni, C. Sangregorio, T. Sen, J. Magn. Magn. Mater. 284, 145 (2004)
[20] G. Zhang, Y. Liu, C. Zhang, W. Hu, W. Xu, Z. Li, S. Liang, J. Cao, Y. Wang, J. Nanopart. Res. 11, 2 (2008)